Ishii et al. Earth, Planets and Space (2018) 70:19
https://doi.org/10.1186/s40623-018-0793-9

Earth, Planets and Space

EXPRESS LETTER

Using Himawari-8, estimation of SO_2 cloud altitude at Aso volcano eruption, on October 8, 2016

Kensuke Ishii[1*], Yuta Hayashi[2] and Toshiki Shimbori[1]

Abstract

It is vital to detect volcanic plumes as soon as possible for volcanic hazard mitigation such as aviation safety and the life of residents. Himawari-8, the Japan Meteorological Agency's (JMA's) geostationary meteorological satellite, has high spatial resolution and sixteen observation bands including the 8.6 µm band to detect sulfur dioxide (SO_2). Therefore, Ash RGB composite images (RED: brightness temperature (BT) difference between 12.4 and 10.4 µm, GREEN: BT difference between 10.4 and 8.6 µm, BLUE: 10.4 µm) discriminate SO_2 clouds and volcanic ash clouds from meteorological clouds. Since the Himawari-8 has also high temporal resolution, the real-time monitoring of ash and SO_2 clouds is of great use. A phreatomagmatic eruption of Aso volcano in Kyushu, Japan, occurred at 01:46 JST on October 8, 2016. For this eruption, the Ash RGB could detect SO_2 cloud from Aso volcano immediately after the eruption and track it even 12 h after. In this case, the Ash RGB images every 2.5 min could clearly detect the SO_2 cloud that conventional images such as infrared and split window could not detect sufficiently. Furthermore, we could estimate the height of the SO_2 cloud by comparing the Ash RGB images and simulations of the JMA Global Atmospheric Transport Model with a variety of height parameters. As a result of comparison, the top and bottom height of the SO_2 cloud emitted from the eruption was estimated as 7 and 13–14 km, respectively. Assuming the plume height was 13–14 km and eruption duration was 160–220 s (as estimated by seismic observation), the total emission mass of volcanic ash from the eruption was estimated as $6.1–11.8 \times 10^8$ kg, which is relatively consistent with $6.0–6.5 \times 10^8$ kg from field survey.

Keywords: Ash RGB, Himawari-8, Atmospheric transport model, SO_2, Aso volcano

Introduction

In an eruption event, in order to estimate the amount of damage promptly, it is important to know the eruption source parameters such as mass eruption rate, plume height and eruption duration. For example, the Japan Meteorological Agency (JMA) operates the Volcanic Ash Fall Forecast (VAFF) system to issue forecasts of areas where ash or lapilli fall is expected around a volcanic eruption (Hasegawa et al. 2015). In this operation, the JMA Regional Atmospheric Transport Model (JMA-RATM) uses initial conditions including total eruption mass which is estimated using the relationship between the total mass and the top height of the plume and eruption duration. In the Volcanic Ash Advisory Center (VAAC) operation, after an eruption, Volcanic Ash Advisories (VAA) are issued at 6-h intervals (normally at 00, 06, 12 and 18 UTC) for as long as an ash cloud is identified in satellite imagery (Tokyo VAAC 2016). For the forecast of volcanic ash by the JMA Global Atmospheric Transport Model (JMA-GATM) in the Tokyo VAAC of the JMA, the top height of ash clouds is an essential parameter.

We can estimate total mass using the relationship between a mass eruption rate and a plume height (e.g., Mastin et al. 2009). However, in some cases, it is not easy to estimate the top height of plumes because meteorological clouds obscure remote cameras and satellite observation.

*Correspondence: kishii@mri-jma.go.jp
[1] Volcanology Research Department, Meteorological Research Institute, 1-1 Nagamine, Tsukuba, Ibaraki 305-0052, Japan
Full list of author information is available at the end of the article

Since weather radar observation is much more sensitive to large particles than small particles such as fine ash or SO_2 gas which are found around the top of the plumes, there are cases in which radar is not useful for estimation of plume height. However, the total eruption mass is sensitive to the top height, and its accurate estimation is indispensable. In addition, for disaster prevention, promptness is vital. Especially, for aviation safety, timely estimation is of great importance. In this context, the Himawari-8 satellite allows very timely volcanic plume monitoring.

Himawari-8, which is a new geostationary meteorological satellite, was put into operation on July 7, 2015 (Bessho et al. 2016). It has significantly advanced features, having sixteen observation bands compared to five in its predecessor. The spatial resolution is 2 km for infrared bands. Furthermore, it has high observation frequencies. Full disk images are taken every 10 min, Japan area images are taken every 2.5 min, and landmark area images are taken every 0.5 min.

For the detection and analysis of volcanic eruptions, one of the most strikingly enhanced points is that the 16 observation bands include new bands #10 (7.3 μm) and #11(8.6 μm) which have sensitivity for SO_2 gas (Watson et al. 2004). Ash RGB (one of the visualization schemes of satellite data; see the "Ash RGB" section for details) using band #11, #13 (10.4 μm) and #15 (12.4 μm) are tricolored satellite images (RGB image) that can discriminate SO_2 clouds and ash clouds from meteorological clouds. The predecessor of Himawari-8 was the Multifunctional Transport Satellite-2 (MTSAT-2, also called Himawari-7), which was also used for the detection and analysis of ash clouds. MTSAT-2 had no bands sensitive to SO_2 gas, so that SO_2 clouds could not be detected, and infrared (IR, 10.8 μm) and a split window (10.8–12.0 μm) were mainly used to discriminate volcanic ash clouds from meteorological clouds (Prata 1989a, b).

In the Japan area, there are other satellites and sophisticated retrieval schemes which have been developed and are available for detection or analysis of volcanic ash or SO_2 clouds. Low Earth orbit satellites provide high-spectral resolution data (Cooke et al. 2014). For example, Yang et al. (2007) developed retrieval of SO_2 from the Ozone Monitoring Instrument (OMI). However, since they are Earth orbit satellites, there are very few chances of observations of ash clouds immediately after an eruption. Geosynchronous satellites provide high temporal resolution allowing detection in near real time (Francis et al. 2012). For geosynchronous satellites, a retrieval algorithm of physical properties of ash cloud (e.g., ash cloud height, optical depth, effective particle radius and mass loading) was developed (Pavolonis and Sieglaff 2010).

On the other hand, the Ash RGB is composite imagery and provides no quantitative information such as the amount of ash or SO_2 in the column and no vertical profile such as the top height of ash or SO_2 clouds. However, because flow of SO_2 clouds depends on the wind field, SO_2 clouds at each altitude flow with different directions and speeds. In this sense, a time series of the Ash RGB should include information of the vertical profile in the atmosphere with vertical wind shear. Therefore, it is possible that vertical information of SO_2 clouds can be obtained from a time series of the Ash RGB and wind field.

In this study, we applied the Ash RGB for the case of SO_2 cloud of the 2016 Aso volcano eruption. The Ash RGB could clearly track the SO_2 cloud from Aso volcano. Furthermore, we estimated the altitude of the SO_2 cloud by comparing the Ash RGB images and the SO_2 numerical simulation results using the JMA-GATM which has processes such as wind advection, gravitational settling, turbulent diffusion and wet/dry deposition. This model is used for volcanic ash forecasts for the safety of aviation services in the Tokyo VAAC operation. Volcanic ash falls by gravitational settling, while the gravitational effect is negligible for SO_2 clouds.

For the SO_2 simulation, we executed the JMA-GATM without gravity settling, in which tracers act as SO_2 cloud. For the estimation of the altitude of SO_2 cloud, we tried a variety of vertical profiles of SO_2 tracers and sought the best initial vertical profile of SO_2 cloud which is consistent with the two-dimensional spread estimated by the Ash RGB images from Himawari-8. In addition, considering pilots' reports and OMI, a limitation of the Ash RGB for the thin SO_2 region was inferred.

Aso volcano

In Japan, there are 111 active volcanos which have erupted within 10,000 years or which have vigorous fumarolic activity. Of these, 50 volcanos were selected by the Coordinating Committee for Prediction of Volcanic Eruption and are constantly monitored by seismometers, tiltmeters, infrasound microphones, remote cameras, etc. (Yamasato et al. 2013). Aso volcano in Kyushu, Japan (Fig. 1) is one of these.

Aso volcano, including Aso caldera and post-caldera central cones, is one of the most active volcanos in Japan. Nakadake, one of the central cones, is the only active cone and consists of seven craterlets. Of these, only one crater (called "First Crater") has been active in the past 80 years (JMA and VSJ 2013). Most recently, several ash emissions occurred in 2003–2005, and volcanic gases and ash were emitted in 2014–2016 (e.g., Miyabuchi et al. 2008).

At Nakadake, a phreatomagmatic eruption occurred at 01:46 JST on October 8, 2016. Prior to this eruption, the last explosive eruption including large infrasonic waves

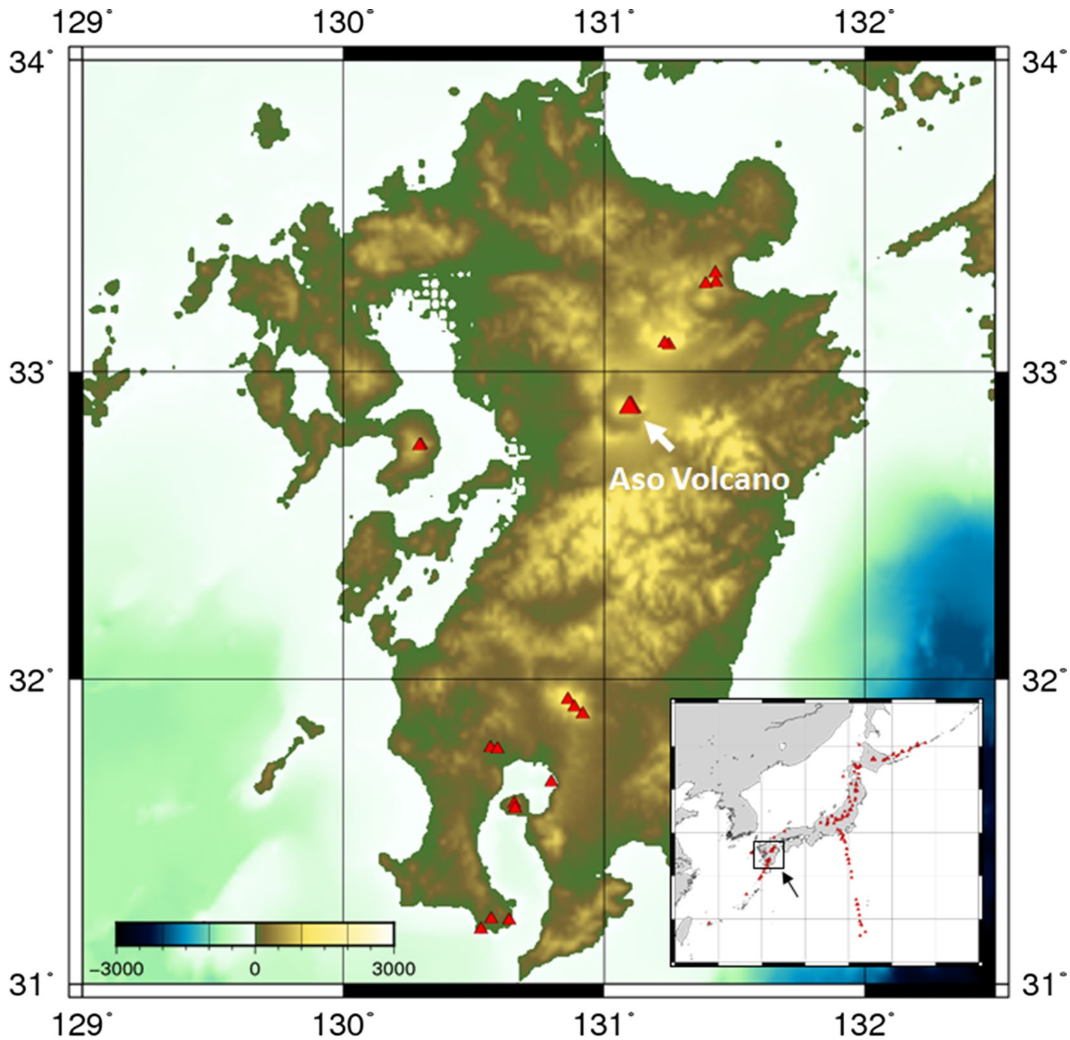

Fig. 1 Map of the Aso volcano. The large triangle indicates Aso volcano. The smaller triangles indicate other volcanos

was January 26, 1980. A seismometer showed that the duration of the eruption was approximately 160–220 s (Fig. 2) (Shimbori 2017).

For the 2016 eruption, because meteorological cloud obscured the remote cameras, the top height of volcanic plumes could not be estimated immediately after the eruption. The Tokyo VAAC issued a VAA with the top height of the plume as 39,000 feet estimated using Infrared (band #13) of Himawari-8 (Tokyo VAAC 2016). In this eruption, ash and lapilli fall spread several kilometers, mainly to the northeast by the ambient wind. For example, lapilli which fell approximately 4.5 km from the vent broke windowpanes, and lapilli which fell approximately 6.5 km away broke more than 1500 solar panels (Sasaki et al. 2017). Further, there were some other effects such as malfunctions of train signals, changes of routes and delays of airplanes, ash fall on crops and damage to agricultural greenhouses. In addition, electricity was cut to 29,000 households around the volcano, and the power outage also caused some disruptions to the water supply.

Ash RGB

When a volcanic eruption occurs, we need to know and understand the details of the eruption as soon as possible for estimating the magnitude of eruption and damage around the volcano, and for predictions such as ash fall forecasts for residents and airborne ash forecasts for aviation safety. For this purpose, we can make the most of Himawari-8. Enhancement of spatial resolution and observation frequencies are very useful for analysis and monitoring of eruption plumes. Compared to MTSAT-2, Himawari-8′s most enhanced point for monitoring

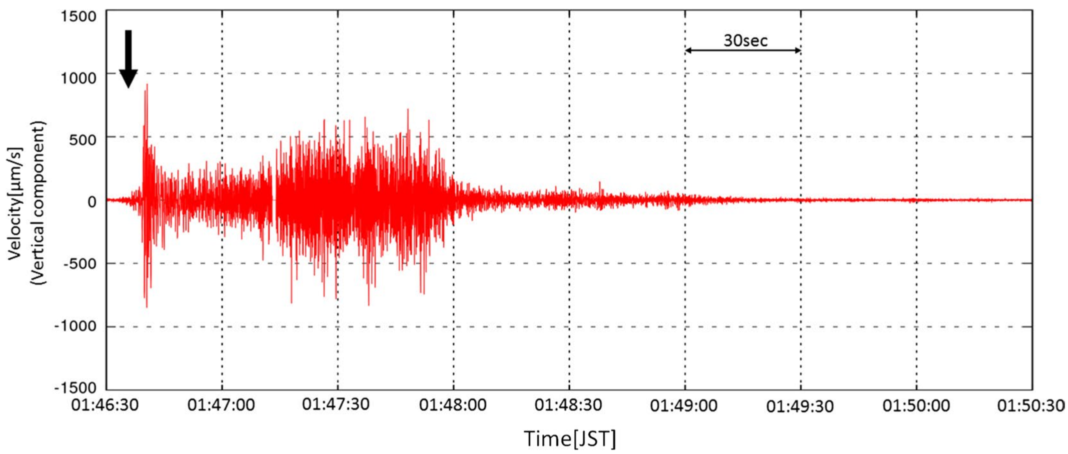

Fig. 2 The volcanic earthquake (vertical component) as measured by a seismogram from Aso volcano eruption, 8 Oct., 2016, 01:46:30–01:50:30JST. The observation point is located approximately 1.2 km west from the vent. The black arrow indicates the eruption time (around 01:46:36JST)

eruption plumes is the addition of bands #10 and #11 which are sensitive to SO_2 gas. These bands enable us to detect "SO_2 rich" plumes which are overlooked by using conventional images such as IR (band #13) and a split window (band #13–#15) for Himawari-8.

In this study, the Ash RGB is based on the report of the Meteorological Satellite Center (2015). It is composed of 3 beams: the RED beam is correlated with the brightness temperature (BT) difference (− 4 to 2 [K]) of band #15 and #13, the GREEN beam is correlated with the BT difference (− 4 to 5 [K]) of band #13 and #11, and the BLUE beam is correlated with band #13(208–243 [K]). In the Ash RGB image, the pinkish color corresponds to ash, and the bright green–yellow color corresponds to SO_2.

Figure 3 shows the Ash RGB images for Aso volcano in this study. The plume which was released from Aso volcano was identified approximately 10 min after eruption from the Ash RGB, and blown eastward while spreading to the north and south by the wind. Within 1 or 2 h after the eruption, the cloud could be tracked by IR (band #13) or the split window even though it was not clear. However, 3 or 4 h after the eruption, the plume could not be tracked. On the other hand, the Ash RGB could track it clearly 12 h after the eruption (see Fig. 5). The color of the Ash RGB in the cloud region indicated SO_2, so that the cloud was presumed to be "SO_2 rich".

Model description and methodology

The numerical simulation provides forecasting of SO_2 clouds by using an initial condition (i.e., initial SO_2 distribution for the numerical model). However, the simulation result depends on the accuracy of the initial conditions. If the initial conditions are not set accurately, the numerical simulations will provide an inaccurate forecast. Conversely, initial conditions providing a forecast which is consistent with observations should have realistic initial distribution. In this case, a simulation result using realistic top and bottom height of SO_2 clouds for the initial conditions of the model should be consistent with the Ash RGB images.

In this study, the numerical simulations of SO_2 clouds are performed by the JMA-GATM which is based on Iwasaki et al. (1998). The JMA-GATM is a Lagrangian model which calculates the time evolution of location of many tracer particles as volcanic ash particles. Each particle's displacement during 1 time step δt is as follows:

$$x(t+\delta t) = x(t) + \bar{u}\delta t + \Gamma\sqrt{2K_{\mathrm{h}}\delta t} \quad (1)$$

$$y(t+\delta t) = y(t) + \bar{v}\delta t + \Gamma\sqrt{2K_{\mathrm{h}}\delta t} \quad (2)$$

$$z(t+\delta t) = z(t) + \bar{w}\delta t + \sum_{\delta t'}\Gamma\sqrt{2K_{\mathrm{v}}\delta t'} - V_{\mathrm{g}}\delta t \quad (3)$$

where $x(t), y(t), z(t)$ are the locations at the time t, and $\bar{u}, \bar{v}$ are wind velocities at the tracer location. $\bar{w}$ is vertical wind which is calculated diagnostically from horizontal divergence of $\bar{u}, \bar{v}$. The third terms in each equation represent sub-grid scale deviations of horizontal and vertical wind. K_{h}, K_{v} are horizontal and vertical diffusion coefficients, and Γ is random displacement whose statistical distribution takes the Gaussian distribution function with mean 0 and standard deviation 1. V_{g} is the terminal fall velocity, which mainly depends on the size of the tracer.

The wind velocities $\bar{u}, \bar{v}, \bar{w}$ are included in the meteorological field predicted by the Global Spectral Model (JMA-GSM) (JMA 2013) for numerical weather prediction. Horizontal and vertical diffusions are formulated

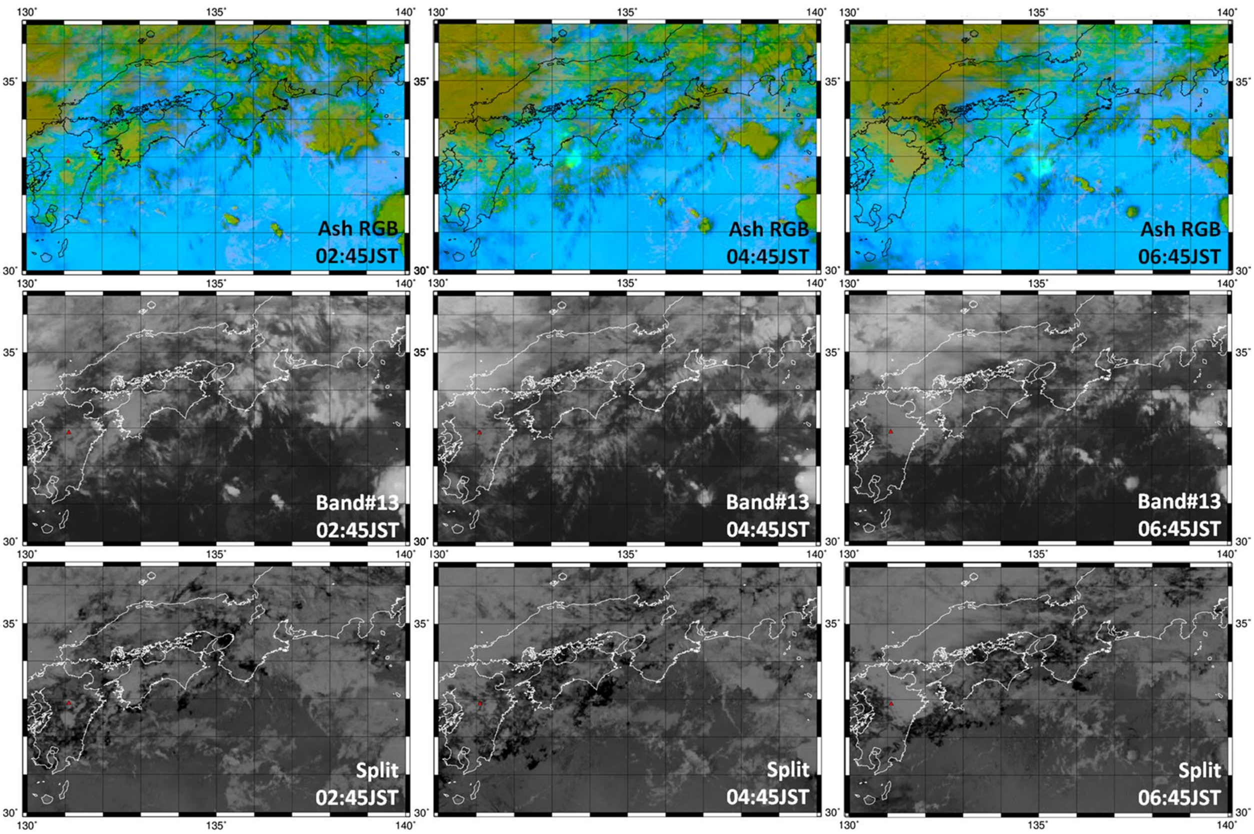

Fig. 3 The Ash RGB (upper row), band #13 image (middle row) and split window (band #13–#15) image (bottom row). The left column is 02:45JST (approximately 1 h after eruption), the center column is 04:45JST (approximately 3 h after eruption), and the right column is 06:45JST (approximately 5 h after eruption)

assuming the random walk model, in which the probability density of the displacements is Gaussian distribution with $\Gamma\sqrt{2K_h\delta t}$ for horizontal diffusion with $K_h = 4.0 \times 10^3$ m^2/s and $\Gamma\sqrt{2K_v\delta t'}$ for vertical diffusion. For the vertical diffusion, K_v is based on Louis et al. (1982), $\delta t'$ is divided into a smaller value than δt. Wet and dry deposition processes are included in the JMA-GATM. The tracers are scavenged by the wet/dry deposition process. Actually, wet deposition includes washout (below-cloud scavenging) and rainout (in-cloud scavenging). However, the JMA-GATM includes only washout which scavenges the tracer using precipitation calculated from JMA-GSM. Tracers near the surface are scavenged by dry deposition which calculates deposition velocity from aerodynamic resistance (Kitada et al.1986). The gravitational settling is calculated based on Suzuki (1983).

In this numerical simulation, 10,000 tracers in the JMA-GATM as SO_2 tracers are set above Aso volcano as a straight line source from bottom height to top height for 3 min from the eruption time, 01:46JST 8 October 2016 (FT = 0 h), and simulations were done up to 15 h after the eruption. In this simulation, an initial vertical profile of SO_2 cloud is used with a bottom height of 2–16 km (every 1 km) and top height 5–17 km (every 1 km), i.e., 2–5, 2–6 km, etc., up to 2–17 km. This was repeated for every new bottom and top height in increments of 1 km; therefore, the final vertical profile was 16–17 km. Considering that the top height is larger than the bottom height, the total number of experiments is 117.

The meteorological fields of the JMA-GSM forecast with an initial time of 21JST October 7, 2016 are used. The meteorological fields such as wind, temperature, pressure and precipitation are taken as grid point values every 3 h (00, 03, 06, 09, 12, 15, 18, 21JST). The time step δt in Eqs. (1)–(3) is 600 [s]. For the location of each tracer at each time step, the meteorological field which is used in the processes is interpolated linearly by time and space. Because tracers in the JMA-GATM simulations have the role of SO_2 cloud, the gravitational settling is switched off.

Results of numerical simulations

Representative results of the 117 experiments by the JMA-GATM are shown in Fig. 4. The spread of SO_2 cloud in each result significantly depends on the initial vertical profile. For example, for an initial SO_2 cloud with an altitude of 2–7 km, the cloud was blown and spread widely from north–northeast to east–northeast from the volcano (upper row in Fig. 4). For an initial SO_2 cloud with an altitude of 7–14 km, it was blown and spread more narrowly from east–northeast to east compared to the 2–7 km cloud, but spread north–south (middle row in Fig. 4). For an initial SO_2 cloud with an altitude of 14–17 km, we can see that the cloud was blown to the east while spreading in an east–west direction (bottom row in Fig. 4). These differences are caused by wind direction shear and wind speed shear. That is, at the time of eruption, in lower altitudes such as from the surface to 7 km, the wind direction is north–northeast to east–northeast. On the other hand, at altitudes of 7–14 km, the wind direction is east–northeast to east, and at altitudes of 14–17 km, the wind blows eastward with wind speed shear. These differences between directions of SO_2 cloud at each altitude were seen 20–30 min after eruption and later.

Discussion

Comparing the Ash RGB and the result of the model simulations, SO_2 vertical profiles with 7–13 and 7–14 km altitudes seem to be most likely. The simulation results show that SO_2 cloud under 7 km was blown to the northeast unlike distribution indicated from the Ash RGB (upper row of Fig. 3). However, actually thin SO_2 cloud seemed to be blown under 7 km from other observations (to be discussed below). For the simulations with SO_2 cloud over 14 km, the south end of the cloud was spreading to the east and west by wind speed shear unlike SO_2 cloud deduced from the Ash RGB. Because the SO_2 cloud spread at 7–13 and 7–14 km is very similar, we could not discriminate the top height of 13–14 km.

In the simulations, the north end of the SO_2 cloud reached Kanto, Japan, as did SO_2 cloud observed by the Ash RGB 12 h after eruption. However, in the south of approximately 35° north latitude, the simulation is not similar to the SO_2 cloud of the Ash RGB. The SO_2 cloud

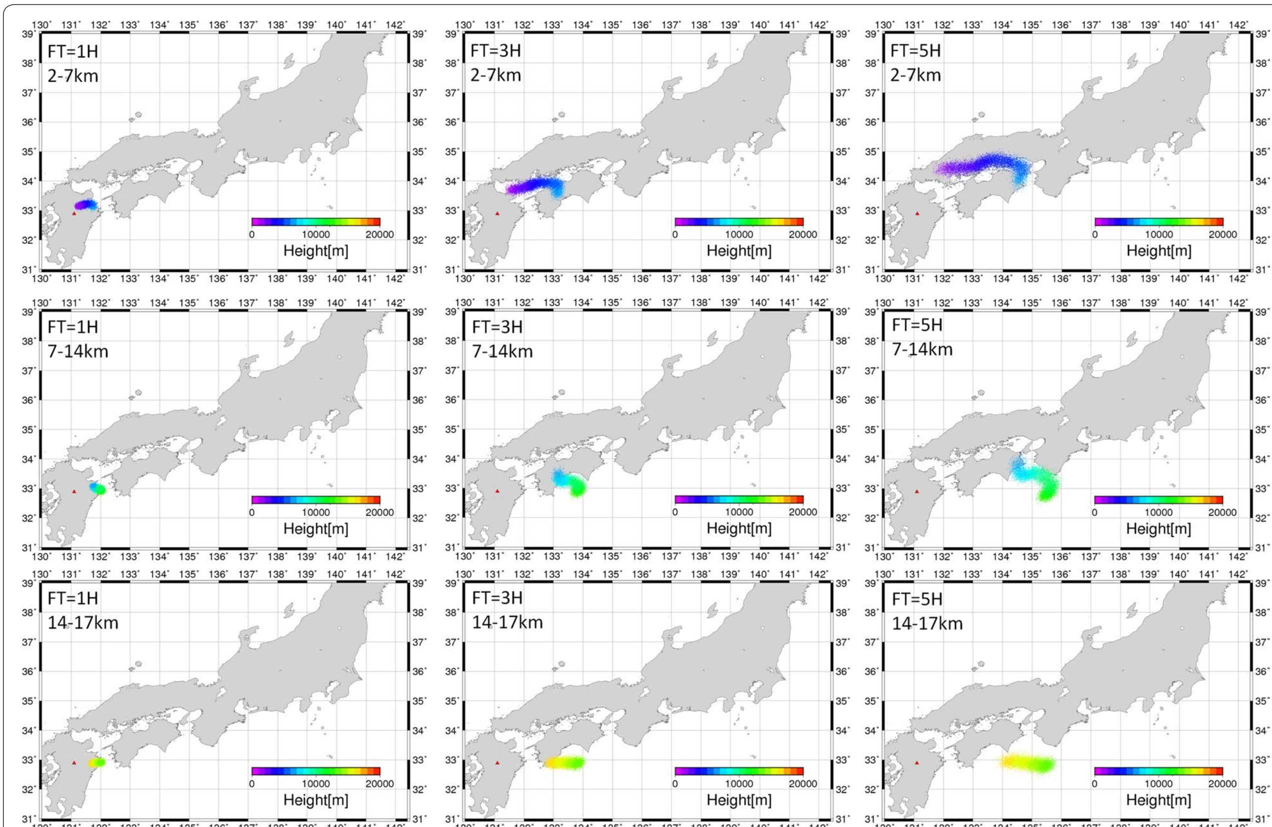

Fig. 4 Results of the SO_2 simulations by JMA-GATM. Upper row: simulation from initial altitude of SO_2 at 2–7 km. Middle row: simulation from initial altitude of SO_2 at 7–14 km. Bottom row: simulation from initial altitude of SO_2 at 14–17 km. The left column is approximately 1 h after eruption (02:46JST). The center column is approximately 3 h after eruption (04:46JST). The right column is approximately 5 h after eruption (06:46JST). The color bar indicates the height [m] of SO_2 tracers

of the Ash RGB is located west of that of the simulation. This difference is possibly caused by the wind of the atmospheric fields.

For further understanding of the results of our simulations, it must be noted that there is uncertainty of the horizontal diffusion coefficient. Because the coefficient depends on the resolution of the meteorological numerical model (Iwasaki et al. 1998), it is difficult to find a universal value. In our study, we determined the coefficient by comparing the Ash RGB and results with some ordered value. However, for a more detailed analysis such as quantitative comparison of ash fall amount around the volcano, the coefficient should be determined more carefully (e.g., Tanaka and Yamamoto 2002).

Comparing the Ash RGB image and the OMI measurements at approximately 12 h after eruption, they are very similar in spread except for the area around the north end of the SO_2 cloud (Fig. 5). That is, OMI detected a more northern region (~ 37° north) of SO_2 than the Ash RGB (~ 35–36° north). For the simulation of an initial profile with an altitude of 5–14 km, the SO_2 cloud spread to the north region like the observation of OMI, unlike the Ash RGB. The locations of pilots' reports which noted the smell of SO_2 are consistent with the simulation of an initial profile with an altitude of 5–14 km (height errors are approximately ± 2 km, except for point h in Fig. 5) and OMI. Therefore, it seems the Ash RGB could not detect the thin SO_2 region under an altitude of 7 km.

We can calculate total mass using the duration of eruption of 160–220 s and a top height 13–14 km using the relationship $H = 2.00 \times \dot{V}^{0.241}$ (Mastin et al. 2009), where H is the top height (km) of the eruption plume, and $\dot{V}$ is the volumetric flow rate (m^3 dense-rock equivalent (DRE) per second). Assuming magma density is 2500 kg/m^3, the total mass of the eruption is 6.1–11.8 × 10^8 kg, which is consistent with field survey 6.0–6.5 × 10^8 kg (Miyabuchi et al. 2017). In addition, the current study estimation of a top height of 13–14 km is also consistent with the JMA-RATM simulation (Shimbori 2017) that showed volcanic ash fall forecast calculated with a top height of 13.1 km

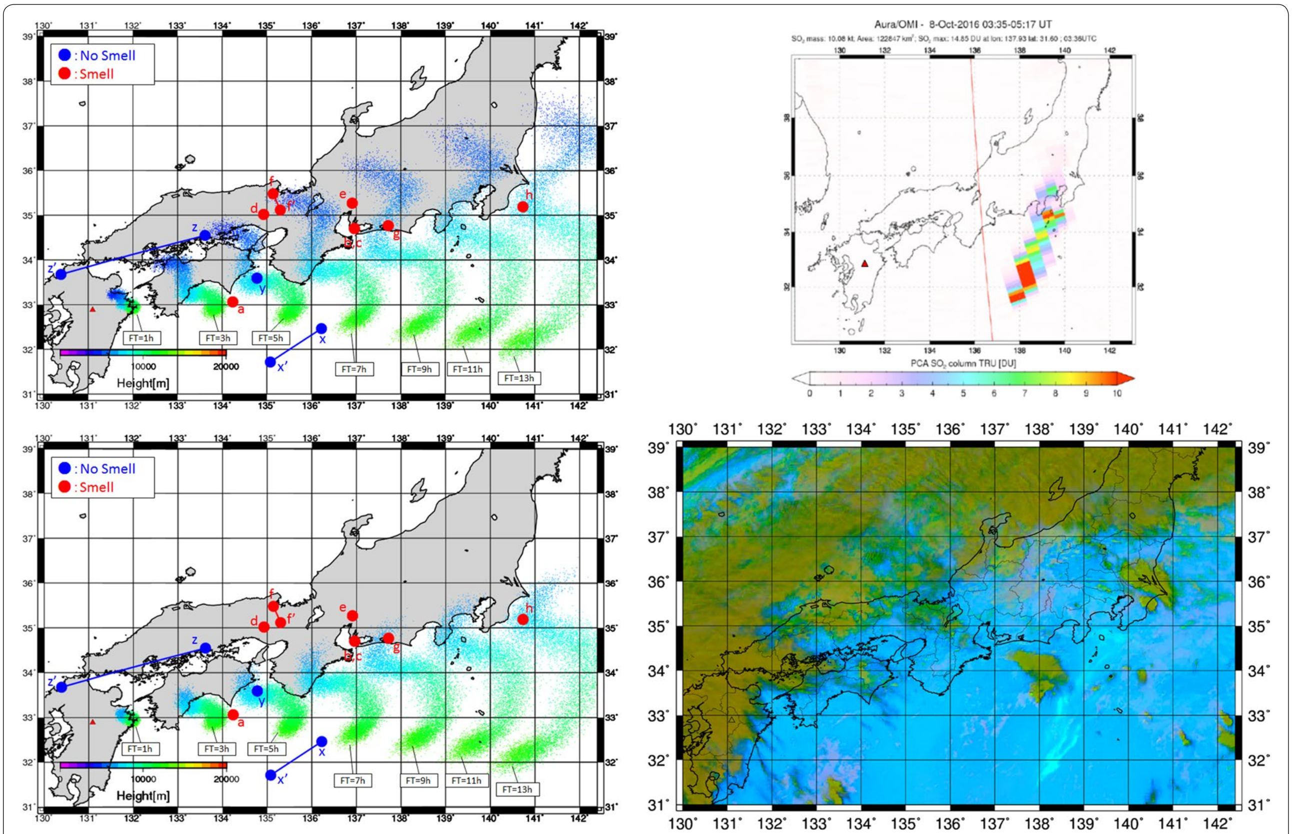

Fig. 5 The two left figures are the time series (FT = 1(02:46JST)-FT13(14:46JST)) of the JMA-GATM simulations and pilots' reports. (The upper figure is the result from an initial altitude of SO_2 at 5–14 km. The bottom figure is the result from an initial altitude of SO_2 at 7–14 km.) The lettered points are pilots' reports including "VA SMELL" or "SULFUR" as follows: a;06:00JST(FL270–320), b;09:16JST(FL210), c;09:34JST(FL210–240), d;09:50JST(FL180), e;10:20JST(FL190), ff';10:28JST(FL090), g;10:39JST(FL290), h;13:32JST(FL090–100), xx';06:08JST(FL370–390), y;08:31JST(FL170), zz';10:40JST(FL360). FL is flight level (FL100 = 10,000 feet). The right upper figure is SO_2 observation from Aura/OMI, 00:35–02:17JST (NASA-GFSC et al. 2016). The right bottom figure is the Ash RGB at 12:46JST

is most consistent with ash fall distribution observation. Therefore, the current simulation results are consistent with both field survey and previous simulation results.

Conclusion

A phreatomagmatic eruption of Aso volcano in Kyushu, Japan, occurred at 01:46 JST October 8, 2016. The Ash RGB images using three observation bands of Himawari-8, including the bands sensitive to SO_2, could detect an "SO_2 rich" cloud which could not be detected by conventional IR (band #13) or split window images more than 12 h after the eruption.

In this study, we estimated the altitude at which the SO_2 cloud was blown by comparing the Ash RGB images and the simulation by the JMA-GATM. It is estimated that the height of the SO_2 cloud was 7–13 or 7–14 km. OMI measurements and pilots' reports suggest that the Ash RGB images could not detect thin SO_2 cloud, and thin SO_2 cloud existed at the altitude of 5–7 km.

Using a top height of 13–14 km and an eruption duration of 160–220 s from the volcanic earthquake, the total emission mass of the eruption is estimated as $6.1–11.8 \times 10^8$ kg. It is relatively consistent with $6.0–6.5 \times 10^8$ kg from field survey.

Abbreviations

BT: brightness temperature; JMA: Japan Meteorological Agency; JMA-GATM: JMA Global Atmospheric Transport Model; JMA-RATM: JMA Regional Atmospheric Transport Model; OMI: Ozone Monitoring Instrument; VAA: Volcanic Ash Advisory.

Authors' contributions

KI performed the SO_2 simulations and comparison between observation and simulation results. YH implemented the algorithm of the Ash RGB from Himawari-8 and analyzed them. TS gathered the observation data such as volcanic earthquake and pilots' reports and analyzed them. All authors read and approved the final manuscript.

Authors' information

Kensuke Ishii is a researcher at the Meteorological Research Institute. Yuta Hayashi is an examination officer at the National Personnel Authority. Toshiki Shimbori is a senior researcher at the Meteorological Research Institute.

Author details

[1] Volcanology Research Department, Meteorological Research Institute, 1-1 Nagamine, Tsukuba, Ibaraki 305-0052, Japan. [2] National Personnel Authority, 1-2-3 Kasumigaseki, Chiyoda-ku, Tokyo 100-8913, Japan.

Acknowledgements

The numerical simulations in this study were performed using a Fujitsu FX100 supercomputer system at the Meteorological Research Institute.

Competing interests

The authors declare that they have no competing interests.

Ethics approval and consent to participate

Not applicable.

Publisher's Note

Received: 7 September 2017 Accepted: 29 January 2018
Published online: 06 February 2018

References

Bessho K, Date K, Hayashi M, Ikeda A, Imai T, Inoue H, Kumagai Y, Miyakawa T, Murata H, Ohno T, Okuyama A, Oyama R, Sasaki Y, Shimazu Y, Shimoji K, Sumida Y, Suzuki M, Taniguchi H, Tsuchiyama H, Uesawa D, Yokota H, Yoshida R (2016) An introduction to Himawari-8/9—Japan's new-generation geostationary meteorological satellites. J Meteorol Soc Jpn 94:151–183. https://doi.org/10.2151/jmsj.2016-009

Cooke MC, Francis PN, Millington S, Saunders R, Witham C (2014) Detection of the Grímsvötn 2011 volcanic eruption plumes using infrared satellite measurements. Atmos Sci Lett 15:321–327. https://doi.org/10.1002/asl2.506

Francis PN, Cooke MC, Saunders RW (2012) Retrieval of physical properties of volcanic ash using Meteosat: a case study from the 2010 Eyjafjallajökull eruption. J Geophys Res 117D00:U09. https://doi.org/10.1029/2011jd016788

Hasegawa Y, Sugai A, Hayashi Y, Hayashi Y, Saito S, Shimbori T (2015) Improvements of volcanic ash fall forecasts issued by the Japan Meteorological Agency. J Appl Volcanol 4:2. https://doi.org/10.1186/s13617-014-0018-2

Iwasaki T, Maki T, Katayama K (1998) Tracer transport model at Japan Meteorological Agency and its application to the ETEX data. Atmos Environ 32:4285–4295. https://doi.org/10.1016/S1352-2310(98)00171-X

Japan Meteorological Agency (2013) Outline of the operational numerical weather prediction at the Japan Meteorological Agency, pp 43–61. http://www.jma.go.jp/jma/jma-eng/jma-center/nwp/outline2013-nwp/index.htm. Accessed 19 July 2017

Japan Meteorological Agency and Volcanological Society of Japan (2013) National catalogue of the active volcanoes in Japan. http://www.data.jma.go.jp/svd/vois/data/tokyo/STOCK/souran_eng/menu.htm. Accessed 26 Oct 2017

Kitada T, Carmichael GR, Peters LK (1986) Effects of dry deposition on the concentration-distributions of atmospheric pollutants within land- and sea-breeze circulations. Atmos Environ 20:1999–2010. https://doi.org/10.1016/0004-6981(86)90341-0

Louis JF, Tiedtke M, Geleyn JF (1982) A short history of the PBL parameterization at ECMWF. Workshop on planetary boundary layer parameterization, Shinfield Park, Reading, 25–27 Nov. 1981. Available via DIALOG. https://www.ecmwf.int/en/elibrary/10845-short-history-pbl-parameterization-ecmwf. Accessed 19 July 2017

Mastin LG, Guffanti M, Servanckx R, Webley P, Barsotti S, Dean K, Durant A, Ewert JW, Neri A, Rose WI, Schneider D, Siebert L, Stunder B, Swanson G, Tupper A, Volentik A, Waythomas CF (2009) A multidisciplinary effort to assign realistic source parameters to models of volcanic ash-cloud transport and dispersion during eruptions. J Volcanol Geotherm Res 186:10–21. https://doi.org/10.1016/j.jvolgeores.2009.01.008

Meteorological Satellite Center (2015) Ash RGB detection of volcanic ash. http://www.data.jma.go.jp/mscweb/en/VRL/VLab_RGB/materials/RGB-Ash-Detection_of_Volcanic_Ash.pdf. Accessed 19 July 2017

Miyabuchi Y, Ikebe S, Watanabe K (2008) Geological constraints on the 2003–2005 ash emissions from the Nakadake crater lake, Aso Volcano, Japan. J Volcanol Geotherm Res 178:169–183. https://doi.org/10.1016/j.jvolgeores.2008.06.025

Miyabuchi Y, Maeno F, Nakada S, Nagai M, Iizuka Y, Hoshizumi H, Tanaka A, Itoh J, Kawanabe Y, Oishi M, Yokoo A, Ohkura T (2017) The October 7–8, 2016 eruptions of Nakadake crater, Aso Volcano, Japan and their deposits. Abstract of Japan Geoscience Union—American Geoscience Union Joint Meeting 2017: SVC47-11. https://confit.atlas.jp/guide/event-img/jpguagu2017/SVC47-11/public/pdf?type=in. Accessed 19 July 2017

NASA-GFSC, Michigan Technological University, National Institute of Advanced Industrial Science and Technology, The School of Science at the University of Tokyo (2016) Amount of SO_2 from Aso eruption, 8th Oct, 2016. https://www.gsj.jp/hazards/volcano/kazan-bukai/yochiren/aso_20161011_2.pdf. Accessed 19 July 2017 **(in Japanese, with English captions)**

Pavolonis M, Sieglaff J (2010) GOES-R Advanced Baseline Imager (ABI) Algorithm theoretical basis document for volcanic ash (detection and height).

Version 2.0, NOAA NESDIS Center for Satellite Applications and Research. Available via DIALOG. http://www.goes-r.gov/products/baseline-volcanic-ash.html. Accessed 19 July 2017
Prata AJ (1989a) Observations of volcanic ash clouds in the 10–12 μm window using AVHRR/2 data. Int J Remote Sens 10:751–761. https://doi.org/10.1080/01431168908903916
Prata AJ (1989b) Infrared radiative transfer calculations for volcanic ash clouds. Geophys Res Lett 16:1293–1296. https://doi.org/10.1029/GL016i011p01293
Sasaki H, Naruke S, Chiba T (2017) Characteristics of damage caused by lapilli fall of the October 8, 2016 eruption of Aso volcano, Japan. Abstract of Japan Geoscience Union—American Geoscience Union Joint Meeting 2017: SVC49-11. https://confit.atlas.jp/guide/event-img/jpguagu2017/SVC49-11/public/pdf. Accessed 19 July 2017
Shimbori T (2017) Volcanic ash and lapilli blowing in the wind. Wind Eng JAWE 42:261–272 **(in Japanese)**
Suzuki T (1983) A theoretical model for dispersion of Tephra. In: Shimozuru D, Yokoyama I (eds) Arc volcanism, physics and tectonics. Terra Scientific Publishing Company, Meguro, pp 95–113
Tanaka HL, Yamamoto K (2002) Numerical simulation of volcanic plume dispersal from Usu volcano in Japan on 31 March 2000 using PUFF model. Earth Planets Space 54:743–752. https://doi.org/10.1186/BF03351727
Tokyo VAAC (2016) Volcanic ash advisories text of 17:56 UTC, 07 Oct. 2016 ASOSAN 2016/8. http://ds.data.jma.go.jp/svd/vaac/data/Archives/2016_vaac_list.html. Accessed 19 July 2017
Watson IM, Realmuto VJ, Rose WI, Prata AJ, Bluth GJS, Gu Y, Bader CE, Yu T (2004) Thermal infrared remote sensing of volcanic emissions using the moderate resolution imaging spectroradiometer. J Volcanol Geotherm Res 135:75–89. https://doi.org/10.1016/j.jvolgeores.2003.12.017
Yamasato H, Funasaki J, Takagi Y (2013) The Japan Meteorological Agency's volcanic disaster mitigation initiatives. Technical Note of the National Research Institute for earth science and disaster prevention 380:101–107. http://vivaweb2.bosai.go.jp/v-hazard/pdf/03E.pdf. Accessed 19 July 2017
Yang K, Krotkov NA, Krueger AJ, Carn SA, Bhartia PK, Levelt PF (2007) Retrieval of large volcanic SO_2 columns from the Aura Ozone Monitoring Instrument: comparison and limitations. J Geophys Res 112D24:S43. https://doi.org/10.1029/2007jd008825